Supporting information for

Atomic Periodic Engineering Enabled Ultrathin High-Efficiency $AgBiS_2$ Solar Cells

Xue Liu, Hongbin Xiao, * Zhigang Zang, and Ru Li*

Key Laboratory of Optoelectronic Technology & Systems (Ministry of Education), College of Optoelectronic Engineering, Chongqing University, Chongqing 400044, China.
*Corresponding authors.
Email: xiaohongbin@cqu.edu.cn, ru.li@cqu.edu.cn

Calculation details

Structure Construction and Geometry Optimization: $AgBiS_2$ crystal structures with different space groups are constructed by VESTA 3.5.7,[1] whose lattice vectors and atom positions are optimized by using the projected augmented wave (PAW) method and the Perdew–Burke–Ernzerhof generalized gradient approximation (PBE-GGA) that are implemented in the Vienna ab initio simulation package (VASP 6.1.1).[2-5] The cutoff energy of 520 eV, and the tolerance of 10^{-6} eV for the SCF cycle are set. The atomic force is set to be smaller than 0.02 eV $Å^{-1}$ during the geometrical optimization. Γ-centered $6 \times 6 \times 4$, $9 \times 9 \times 1$, and $4 \times 4 \times 2$ points with k-spacing of $2\pi \times 0.04$ $Å^{-1}$ are used to sample the Brillouin zone of tetra-P4/mmm, trigon-$R\bar{3}m$ and tetra-$I4_1$/amd $AgBiS_2$, respectively. Open-source code VASPKIT 1.3.5 is used to prepare the input files.[6]

Ab Initio Molecular Dynamics Simulations. AIMD simulations of tetra-P4/mmm, trigon-$R\bar{3}m$ and tetra-$I4_1$/amd $AgBiS_2$ are carried out with a $3 \times 3 \times 3$ supercell using the PAW method and the PBE-GGA implemented in VASP 6.1.1. The canonical ensemble (*NVT*) with a Nose-Hoover thermostat is used to control the temperature during the simulation. AIMD has been run for 5 ps with temperature of 300 K and the time step of 1 fs, the atomic trajectory data every 10 fs are collected to analysis the pair correlation function. The other basic parameters are in agreement with that of the geometrical optimizations.

Phonon dispersion calculations. The phonon dispersion of tetra-P4/mmm, trigon-$R\bar{3}m$ and tetra-$I4_1$/amd $AgBiS_2$ are carried out are performed by force constants method (VASP-DFPT) implemented in the PHONOPY code. The energy cutoff is increased to

800 eV, and high symmetry points is selected from the suggestion from online tools Seek-Path.

Electronic and Optical Calculations: Hybrid functional HSE06+SOC is used to calculate the electronic band structure of the tetra-P4/mmm, trigon-$R\bar{3}m$ and tetra-$I4_1$/amd $AgBiS_2$, respectively. Effective mass of the electron and hole is obtained by Python code Effmass,[7] and the Wannier-Mott exciton binding energy is calculated according to $\mu R_y/m_0\varepsilon_r^2$, where is R_y the Rydberg unit of energy, ε_r is the static dielectric constant, $\mu = (m_e^* m_h^*)/(m_e^* + m_e^*)$ is the reduced mass of the electron and hole, m_0 is the electron mass. The frequency dependent dielectric constant is computed within the framework of Random-Phase-Approximation (RPA) utilizing HSE06 eigenvalues and eigenfunctions. VASPKIT code is used to post process the linear optical properties from the frequency-dependent complex dielectric function. Shockley Queisser limited efficiency data is adopted from reference[8] and replotted for comparison.

Spectroscopic Limited Maximum Efficiency (SLME) calculation: The SLME was introduced by Yu and Zunger, [9] where it gives the theoretical efficiency of a material that depends mainly on two parameters. First, the band gap and the nature of the band gap of the material, and second the optical absorption coefficient of the material. The absorption coefficient gives us the penetration depth of a photon with particular energy before which it can get absorbed by the material. The SLME (η) is defined as

$$\eta = \frac{P_m}{P_{in}}$$

where P_m is the maximum power density, and P_{in} is the incident power density from the solar spectrum. The J-V characteristic of the solar cell gives the maximum power density for the SLME.

$$P = JV = (J_{sc} - J_0(e^{\frac{eV}{kT}} - 1))V$$

where J and V are the total current density and potential over the absorber layer, respectively. k is Boltzmann's constant, T is the temperature, and e is the elementary charge. J_{sc} and J_0 are the short-circuit current density and reverse saturation current density, respectively. The absorption coefficient of the material $\alpha(\omega)$, the AM1.5G solar spectrum $I_{sun}(E)$, and the black-body spectrum $I_{bb}(E,T)$ define the J_{sc} and J_0.

$$J_{sc} = e\int_0^\infty \alpha(\omega) I_{sun}(E) dE$$

$$J_0 = \frac{J_0^r}{f_r} = \frac{e\pi}{f}\int_0^\infty \alpha(\omega) I_{bb}(E,T)dE$$

J_0^r is the radiative recombination current density, and f_r is the fraction of radiative recombination, which is defined by the following equation.

$$f_r = exp^{[r0]}(\frac{E_g^{da} - E_g}{kT})$$

where E_g and E_g^{da} are the fundamental and direct allowed band gap, respectively. We used the VASPKIT code for post-processing of the VASP calculated data, and the SLME is calculated by VASPKIT 1.3.5.

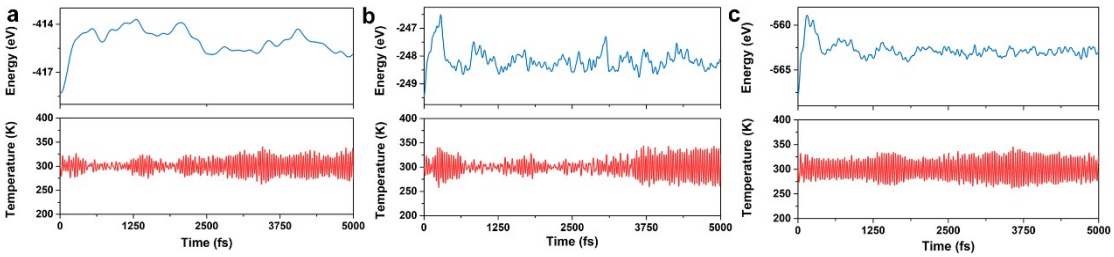

Figure S1. Energy and temperature during the simulation of (a) tetra-P4/mmm, (b) trigon-R$\bar{3}$m and (c) tetra-I4$_1$/amd $AgBiS_2$ structures.

Table S1. Structure features, formation energy (ΔE, eV/atom), energy bandgap (E_g at HSE06+SOC level) and the nature of electronic band structure of the proposed $AgBiS_2$ structures.

	Structure features	**ΔE(eV)**	**E_g(eV)**	**Type**
tetra-P4/mmm	Four edge shared BiS_6 octahedron	0	0	Metallic
trigon-R$\bar{3}$m	Six edge shared titled BiS_6 octahedron	-0.104	1.118	Indirect bandgap
tetra-I4$_1$/amd	Three edge shared intertwined BiS_6 octahedron	-0.059	0.972	Direct bandgap

Table S2. Calculated effective carrier mass m^*, Wannier-Mott exciton binding energy E_b, static dielectric constant ε_r that contributed by ionic (ε_{ion}) and electronic (ε_∞) of semiconducting $AgBiS_2$.

	m^*/m_0	E_b (meV)	ε_{ion}	ε_∞	ε_r
trigon-$R\bar{3}m$	0.7397(h)	0.15	96.18(*XX/YY*)	19.43(*XX/YY*)	115.61(*XX/YY*)
	0.1929(e)	1.62	22.64(*ZZ*)	12.44(*ZZ*)	35.08(*ZZ*)
tetra-$I4_1$/amd	0.8575(h)	0.34	61.62(*XX/YY*)	57.70(*XX/YY*)	119.32(*XX/YY*)
	0.6320(e)	0.0047	991.63(*ZZ*)	25.43(*ZZ*)	1017.06(*ZZ*)

*These are traces of dielectric tensors

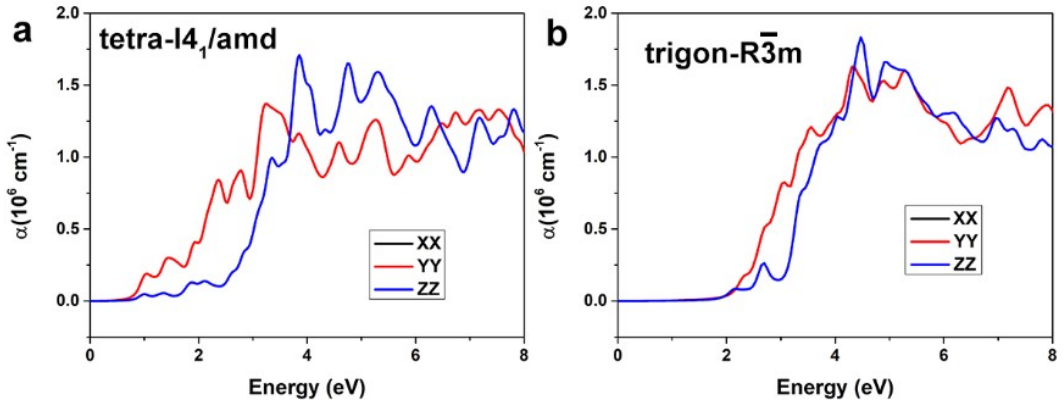

Figure S2. Calculated *XX/YY/ZZ* components absorption coefficient of anisotropic (a) tetra-$I4_1$/amd and (b) trigon-$R\bar{3}m$ $AgBiS_2$.

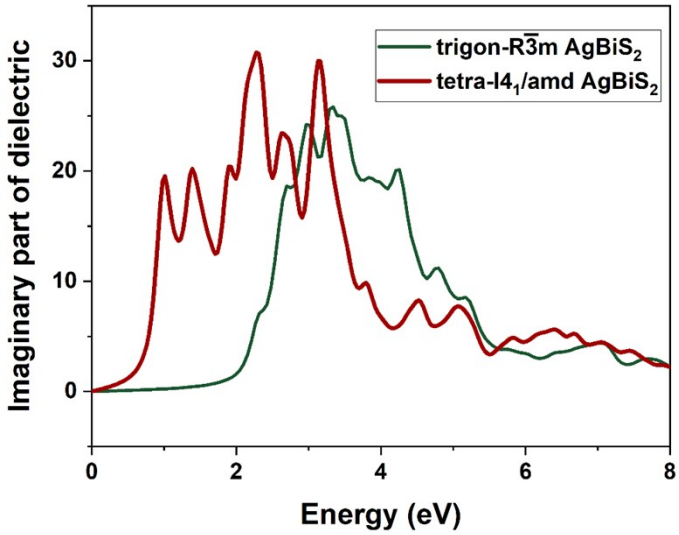

Figure S3. Calculated imaginary part of dielectric constant for tetra-$I4_1$/amd and trigon-$R\bar{3}m$ $AgBiS_2$.

Reference

1. Momma K, Izumi F. VESTA 3 for three-dimensional visualization of crystal, volumetric and morphology data. Journal of applied crystallography 2011, **44**(6)**:** 1272-1276.
2. Blöchl PE. Projector augmented-wave method. Physical Review B 1994, **50**(24)**:** 17953-17979.
3. Kresse G, Furthmüller J. Efficient iterative schemes for ab initio total-energy calculations using a plane-wave basis set. Physical Review B 1996, **54**(16)**:** 11169-11186.
4. Kresse G, Joubert D. From ultrasoft pseudopotentials to the projector augmented-wave method. Physical Review B 1999, **59**(3)**:** 1758-1775.
5. Perdew JP, Burke K, Ernzerhof M. Generalized gradient approximation made simple. Physical review letters 1996, **77**(18)**:** 3865.
6. Wang V, Xu N, Liu J-C, Tang G, Geng W-T. VASPKIT: A user-friendly interface facilitating high throughput computing and analysis using VASP code. Computer Physics Communications 2021, **267:** 108033.
7. D. Whalley L. effmass: An effective mass package. Journal of Open Source Software 2018, **3**(28)**:** 797.
8. Rühle S. Tabulated values of the Shockley–Queisser limit for single junction solar cells. Solar Energy 2016, **130:** 139-147.
9. Yu L, Zunger A. Identification of Potential Photovoltaic Absorbers Based on First-Principles Spectroscopic Screening of Materials. Physical Review Letters 2012, **108**(6)**:** 068701.